BI-METAL INJECTION MOLDING OF
TOUGH/WEAR-RESISTANT COMPONENTS

John L. Johnson, Lye King Tan,* Ravi Bollina,**
Pavan Suri** and Randall M. German**

AMTellect, Inc., State College, PA 16801
*Advanced Materials Technologies Pte Ltd, Singapore 609602
**The Pennsylvania State University, University Park, PA 16802

ABSTRACT

Bi-material components can be processed by MIM by two-color injection molding and co-sintering, but compositions and sintering cycles must be optimized to minimize shrinkage mismatch while providing the desired properties. The effects of sintering temperature on the sintered density, hardness, and mechanical properties of M2 tool steel and boron-containing 316L stainless steel are investigated. The compatibility of co-sintering these materials is predicted based on calculations of the thermal stress and *in situ* strength of the component during sintering. This prediction is verified by successful Bi-MIM processing of 316L-0.5B stainless steel/M2 tool steel components for applications that require a combination of toughness and wear resistance.

INTRODUCTION

To date, MIM applications have been mostly restricted to monolithic materials such as low-alloy steels, stainless steels, tungsten alloys, titanium, or controlled expansion alloys such as Kovar or Invar. After fabrication, the MIM product is usually combined with another component to form an assembly. Since sintering is performed at temperatures where diffusion bonding is possible, a recent goal in MIM has been to form green assemblies (join prior to sintering) and use the sintering step for diffusion bonding.

Most recently, a further evolution has taken place where the green assembly is performed directly in molding using a technology known as bi-metal injection molding (Bi-MIM) [1-3]. If two feedstocks of the differing materials can be designed to co-sinter, then two-color plastic molding technology can be employed to form the assembly in the molding step. The intent is to generate bi-material net-shape structures with properties tailored to a wide range of applications, which might include material combinations selected for

    magnetic and non-magnetic
    magnetic response and corrosion resistance
    controlled porosity and high thermal conductivity
    high inertial weight and high strength

high thermal conductivity and low thermal expansion coefficient
wear resistance and high toughness
high thermal conductivity and good glass to metal sealing
high elastic modulus and high damping capacity
magnetic response and electrical resistance.

This paper focuses on the development of bi-material components consisting of M2 tool steel for high hardness and wear resistance combined with 316L austenitic stainless steel for toughness. Processing of bimaterial components requires careful control of the sintering shrinkage of the two materials to ensure densification and bonding while avoiding differential stresses that might induce cracking or distortion. Since M2 gives rapid densification via supersolidus liquid phase sintering within a narrow temperature window, typically 1220-1250°C depending on carbon level [4,5], modifications to the 316L are needed to enhance its sintering over the same temperature range. Boron additions lower the melting temperature of 316L and enhance its densification behavior at lower temperatures [6]. The current study defines the conditions at which M2 and 316L with boron additions can be co-sintered and their resulting properties under these conditions.

EXPERIMENTAL PROCEDURES

The compositions for molding and sintering trials were M2 tool steel, 316L austenitic stainless steel, and 316L-0.5B. Prealloyed powders were used for the standard grades and boron was added to the 316L as an elemental powder. The characteristics of the prealloyed powders are given in Table I.

For dilatometry studies, the powders were mixed with 2 wt.% paraffin in a Turbula mixer for 30 minutes. Cylindrical samples were die pressed and thermally debound in hydrogen at 575°C. Shrinkage during sintering of the debound components was measured with an Anter vertical tube dilatometer. The samples were heated at a rate of 10°C/minute to 1400°C in a 95% argon/5% hydrogen atmosphere.

For injection molding trials, the powders for each composition were mixed with a wax-polymer binder at a solids loading of 65 volume percent. MPIF standard 50 tensile bars and demonstration components were injection molded. The injection molded components were debound by a two-step process. First, the components were solvent debound to remove the wax portion of the binder. Then the parts were thermally debound and presintered by heating to 900°C in a hydrogen atmosphere. The debound components were heated in a Seko graphite vacuum furnace at a rate of 10°C/minute to temperatures ranging from 1225° to 1330°C. The M2 tool steel samples were heat treated in nitrogen by preheating to 800°C, hardening at 1170°C for 5 minutes, air quenching, and single tempering at 550°C for 1 hour. The samples were wrapped in stainless steel foil to prevent decarburization.

Archimedes' technique of water displacement was used for measuring the density of sintered specimens. The tensile strengths were measured using a MTS Systems Corporation Sintech 20/D universal testing machine with a 20000 lb (88.9 kN) load cell in accordance with MPIF Standard 50. Each sample was measured, placed in the tensile fixture, loaded at 2 mm/minute, and monitored for fracture and ultimate tensile loading. The 0.2% offset yield strength was determined from the stress-strain curve. Elongation was measured with a set of calipers. The tensile bar hardness was measured with a Rockwell hardness tester. For microstructural examination, the samples were sectioned, mounted, and polished to 0.3 μm surface finish using standard metallographic procedures. Carbon content was measured with a Horiba EMIA-8200 carbon/sulfur analyzer.

Table I. Powder characteristics

Powder	Pycnometer density (g/cm³)	Apparent density (g/cm³)	Tap density (g/cm³)	D_{10} (µm)	D_{50} (µm)	D_{90} (µm)
316L	7.84	3.03	4.18	3.8	10.2	21.7
M2	8.00	3.46	4.55	3.6	9.8	20.6

RESULTS

Sintering behavior

The sintering behavior of M2 high speed tool steel, 316L austenitic stainless steel, and 316L with 0.5% boron is given in Figure 1. Densification of the M2 occurs very rapidly in the 1225-1245°C range. The densification of 316L begins at a much lower temperature, but occurs slowly. Such widely varying shrinkage rates are not conducive to co-sintering; however, boron additions to 316L increase the shrinkage rate within the same temperature range as the M2, making co-sintering much more feasible.

The sintered densities of M2 and 316L-0.5B bars sintered for 30 minutes at temperatures ranging from 1225 to 1245°C are plotted in Figure 2. After sintering at 1225°C, the density of the 316L-0.5B is more than 15% higher than that of the M2. However, raising the sintering temperature to 1245°C increases the densification rate of the M2 and both compositions achieve greater than 95% of their theoretical density. Thus, Bi-MIM components with these compositions need to be heated to 1245°C to get rapid densification from both materials.
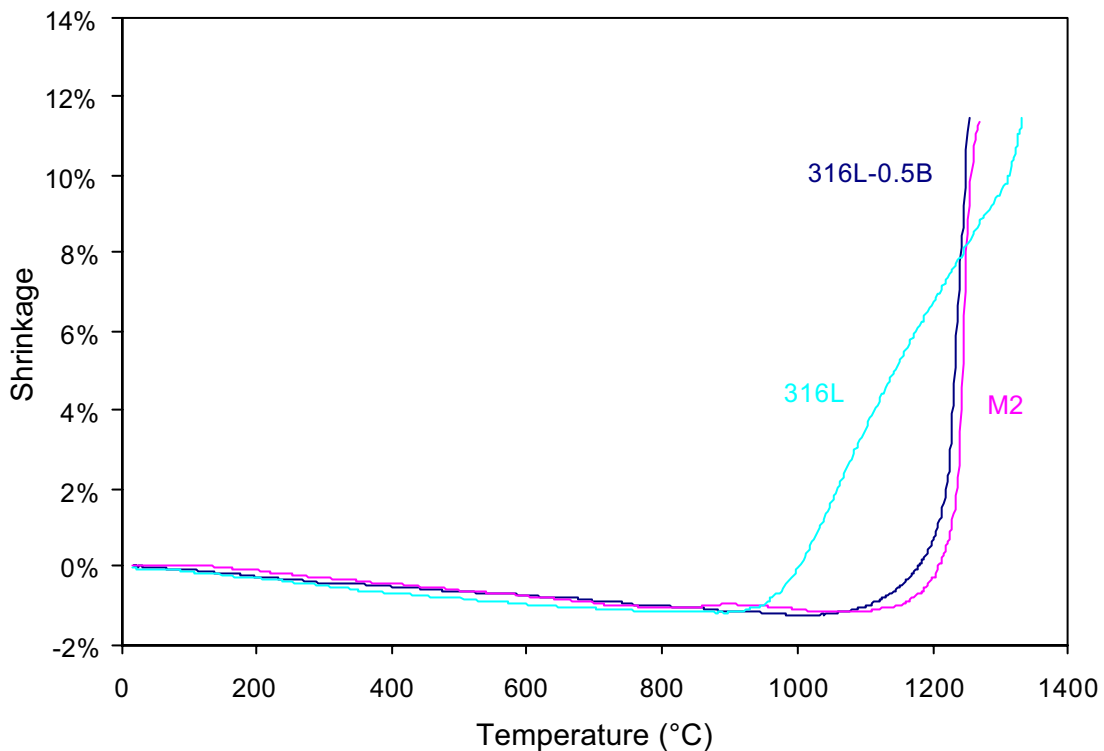

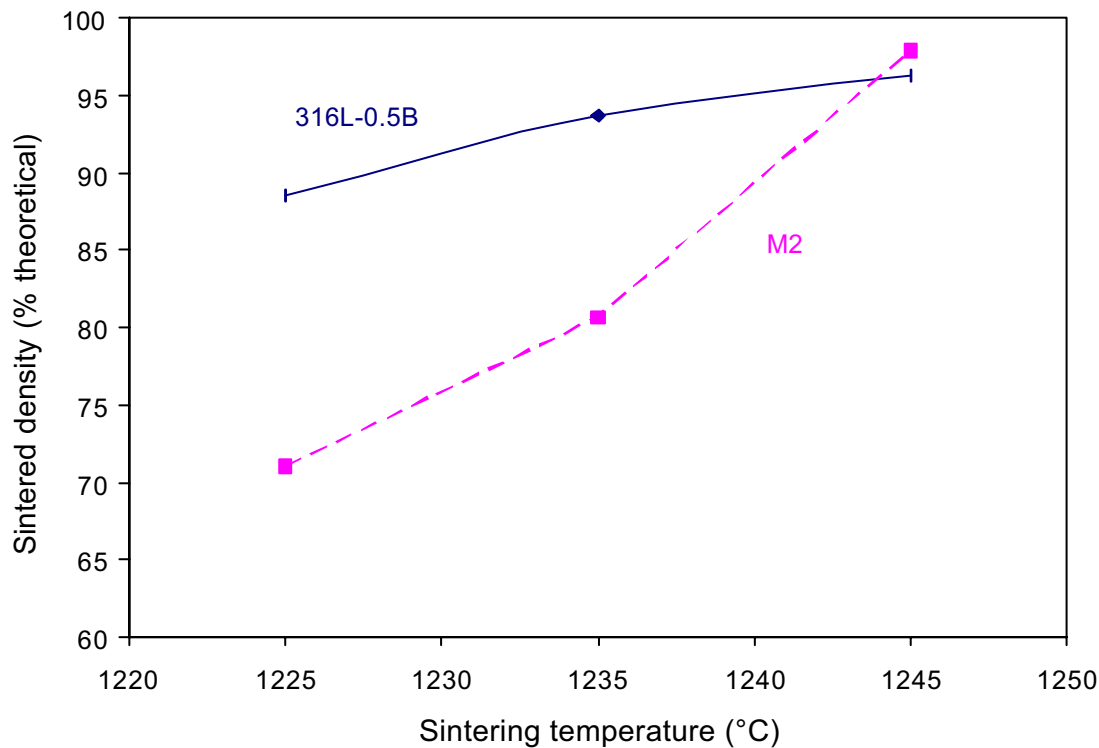Figure 1. Temperature dependence of the shrinkage for M2, 316L, and 316L-0.5B.

Figure 2. Effect of sintering temperature on the density of 316L with 0.5% B and M2 tool steel.

Mechanical properties

The effect of sintering temperature on the ultimate tensile strength and elongation of M2 tool steel is shown in Figure 3. The strength increases with sintering temperature as the density increases and achieves a value of 1480 MPa at 1245°C. Ductility is very limited. Hardness values for the as-sintered and heat treated bars are given in Table II. The as-sintered hardness increases dramatically with sintering temperature. Heat treatment of the bars sintered at 1245°C, increases the hardness from 47 HRC to 59 HRC. The measured carbon content was 0.87%. The carbon content of the powder was 1.08 wt.% so some carbon was lost during processing, but the measured carbon content falls within the lower spec range for M2.

The effect of sintering temperature on the ultimate tensile strength, yield strength, and elongation of 316L-0.5B is shown in Figure 4. The optimal mechanical properties are achieved at 1235°C, although the yield strength is relatively unaffected by the sintering temperature. The ultimate tensile strength and elongation decrease at 1245°C despite the slight increase in sintered density.

The mechanical properties of 316L-0.5B are compared to 316L without boron additions in Table III. The addition of 0.5% boron lowers the sintering temperature by 85°C and slightly improves the yield strength and ultimate tensile strength. Elongation drops with the boron additions, but still shows reasonable ductility.
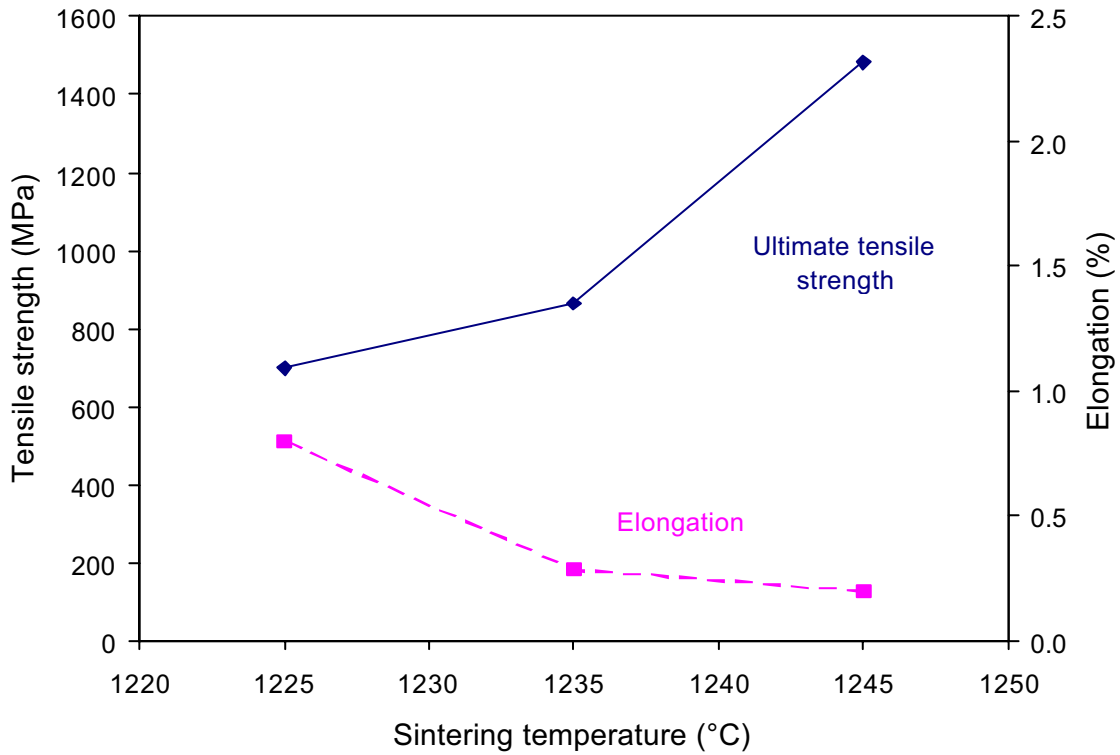
Figure 3. Effect of sintering temperature on the ultimate tensile strength and elongation of M2.

Table II. Effect of sintering temperature on the hardness of as-sintered and heat-treated M2

Sintering temperature (°C)	As-sintered hardness	Heat-treated hardness
1225	42 HRA	-
1235	16 HRC	-
1245	47 HRC	59 HRC

Microstructures

Optical micrographs of 316L-0.5B and M2 after sintering at 1245°C are shown in Figure 5. Pores are evident in the 316L-0.5B sample, which also shows coarse grains and continuous grain boundary films, indicating a higher than optimal sintering temperature. The M2 sample shows a more desirable microstructure with a fine grain size, dispersed carbides, and little porosity.
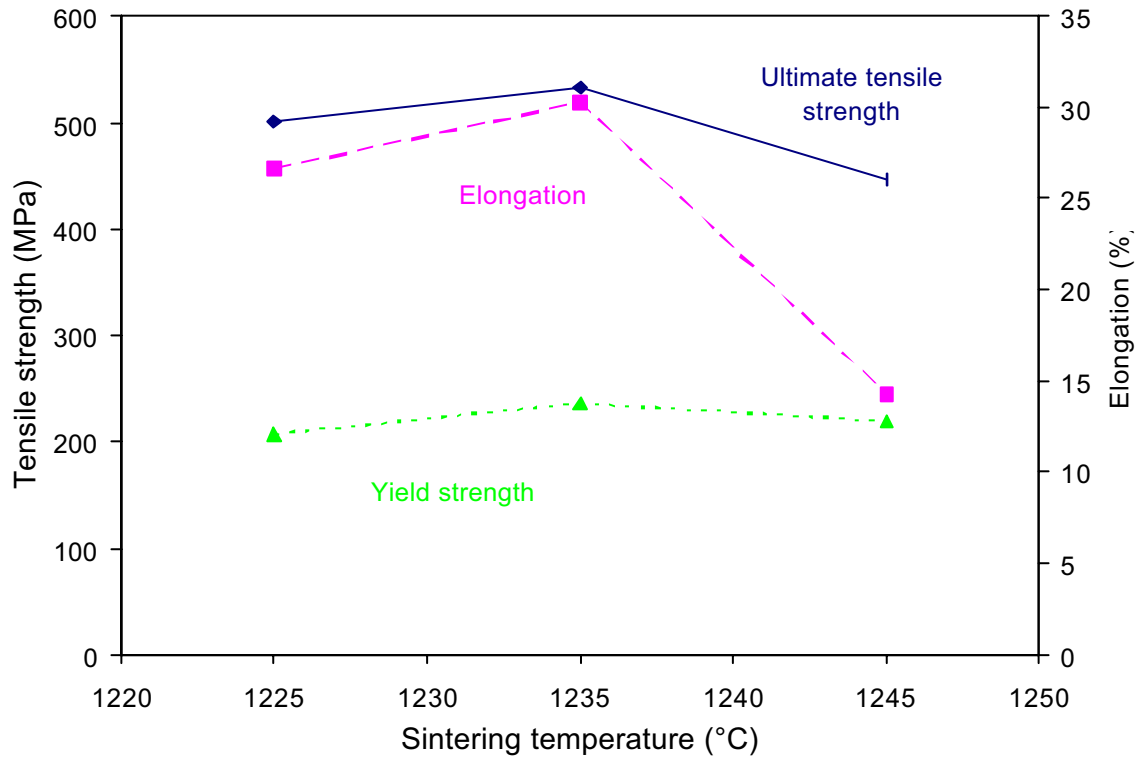
Figure 4. Effect of sintering temperature on the ultimate tensile strength and elongation of 316L-0.5B.

Table III. Effect of boron additions on the sintering temperature and properties of 316L

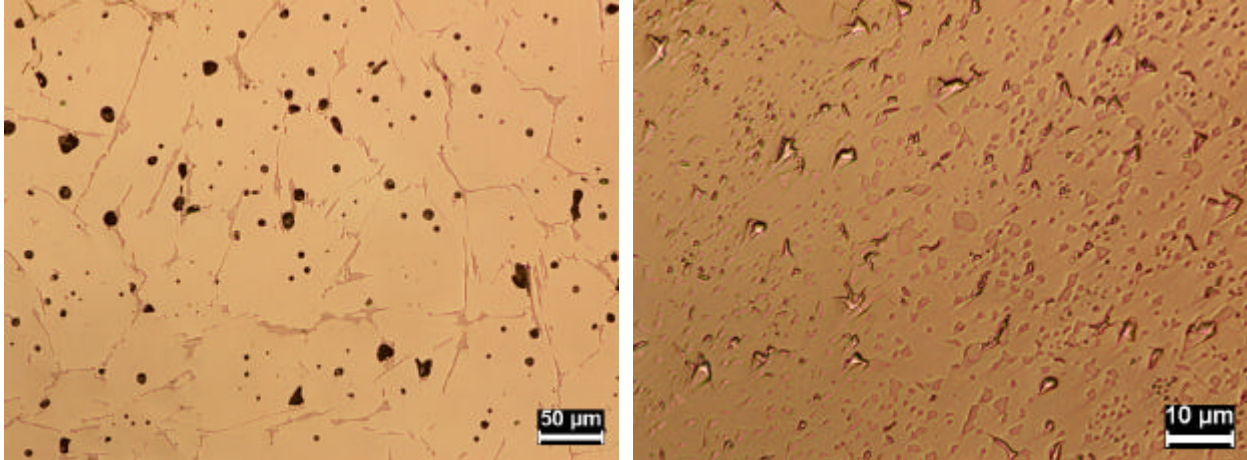|	0% B	0.5% B
Sintering temperature (°C)	1330	1245

Density
    g/cm^3
    % of theoretical
	7.57
	94.6
		7.70
		96.3

Yield strength (MPa)	175	220
Ultimate tensile strength (MPa)	425	450
Elongation (%)	78	14
Hardness (HRB)	46	75

Figure 5. Optical micrographs of 316L-0.5B (left) and M2 (right) after sintering at 1245°C.

CO-SINTERING MODEL

Processing of bimaterial components requires careful control of the sintering shrinkage of the two materials to ensure densification and bonding while avoiding differential stresses that might induce cracking or distortion. For a concentric ring geometry, shrinkage mismatches result in both radial stresses, which are the highest at the interface and lead to interfacial separation, as well as hoop stresses, which lead to radial cracking. These stresses are schematically illustrated in Figure 6 for the case in which the shrinkage of the outer ring is greater than the shrinkage of the inner ring. Interfacial separation is unlikely when good metallurgical compatibility exists between the two components, such as M2 and 316L. However, radial cracking of one or both of the rings can still occur if the hoop stresses arising from shrinkage mismatch exceed the tensile strength of the material. Here, we analyze these stresses and compare them to the intrinsic strengths of the M2 and 316L to predict whether or not bi-material components can be successfully processed.
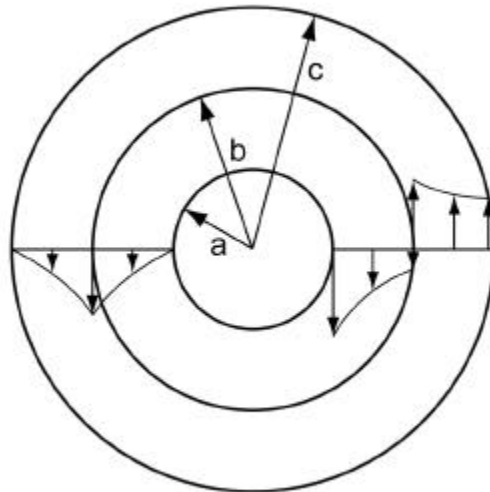

Figure 6. Radial stresses (shown on the left) and hoop stresses (shown on the right) induced in concentric ring components during processing in which the outer ring shrinks more than the inner ring.

Mismatch stresses and material strengths vary throughout the sintering cycle. MIM components loose strength as the binder is removed. They reach a minimum strength once the binder is gone and before initial stage sintering begins. A fortunate happenstance is that when the strength of the component is the lowest, the mismatch stress is often low due to limited dimensional change. As necks develop between particles, their strength increases, reaches a maximum and then decreases as the material thermally softens. During sintering, the *in situ* strength after binder removal is given by [7]

$$\sigma_i = \sigma_y(T) \cdot \frac{N_c \cdot V_s}{k\pi} \cdot \left(\frac{X}{D}\right)^2 \tag{1}$$

where $\sigma_y(T)$ is the temperature dependent yield stress of the bulk material, N_c is the coordination number, V_s is the fractional density, k is a stress concentration factor, X is the neck size, and D is the particle diameter. The coordination number depends on the density, while the stress concentration factor is a function of the X/D ratio, which can be calculated from sintering simulations [7]. A plot of the predicted *in situ* strength of M2 and 316L during heating is given in Figure 7. The *in situ* strength is primarily governed by the increase in the X/D ratio relative to the decrease in the inherent strength of the material.
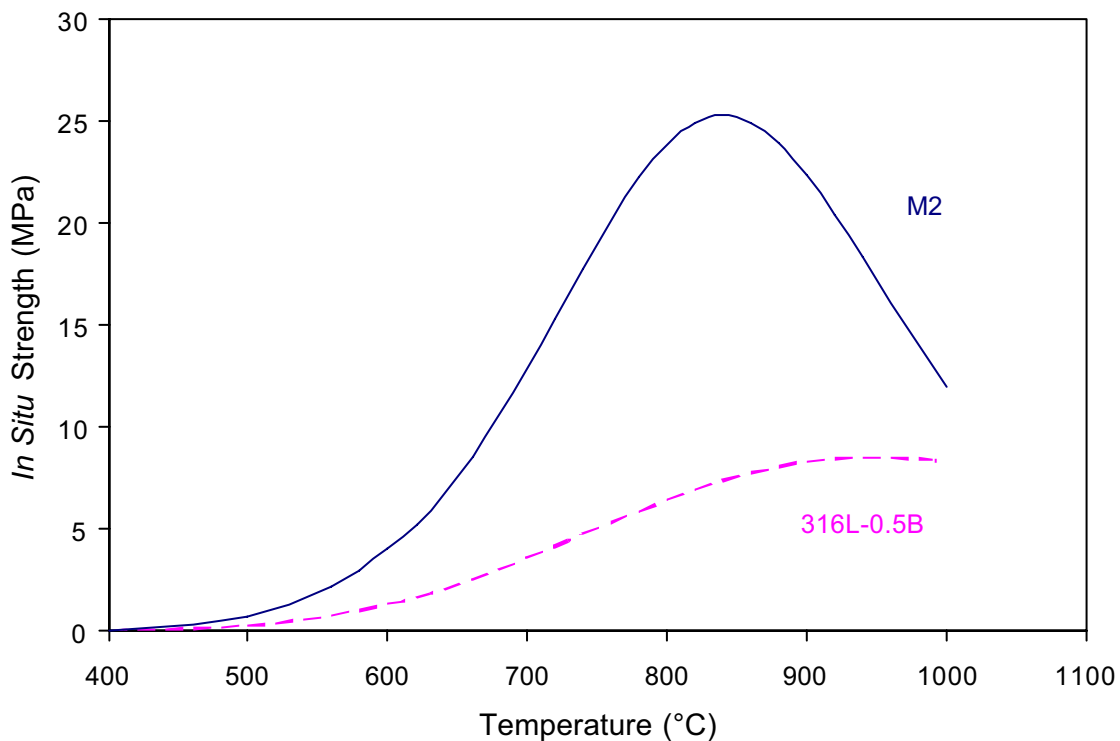

Figure 7. Evolution of the *in situ* strength of M2 and 316L-0.5B with temperature.

The *in situ* strength can be compared to the mismatch stress. As shown in Figure 6, the maximum tensile hoop stress is at the interface if the shrinkage of the outer ring is greater than the shrinkage of the inner

ring. Assuming limited plasticity of the material, the hoop stress in the outer ring at the interface is given by [8]

$$\sigma_{h,outer,max} = \frac{E\delta}{2c}\frac{c^2 - a^2}{b^2 - a^2}\left(1 + \frac{b^2}{c^2}\right) \qquad (2)$$

The elastic moduli of M2 and 316L vary with temperature due to both thermal softening and to decreases in porosity and are plotted in Figure 8.
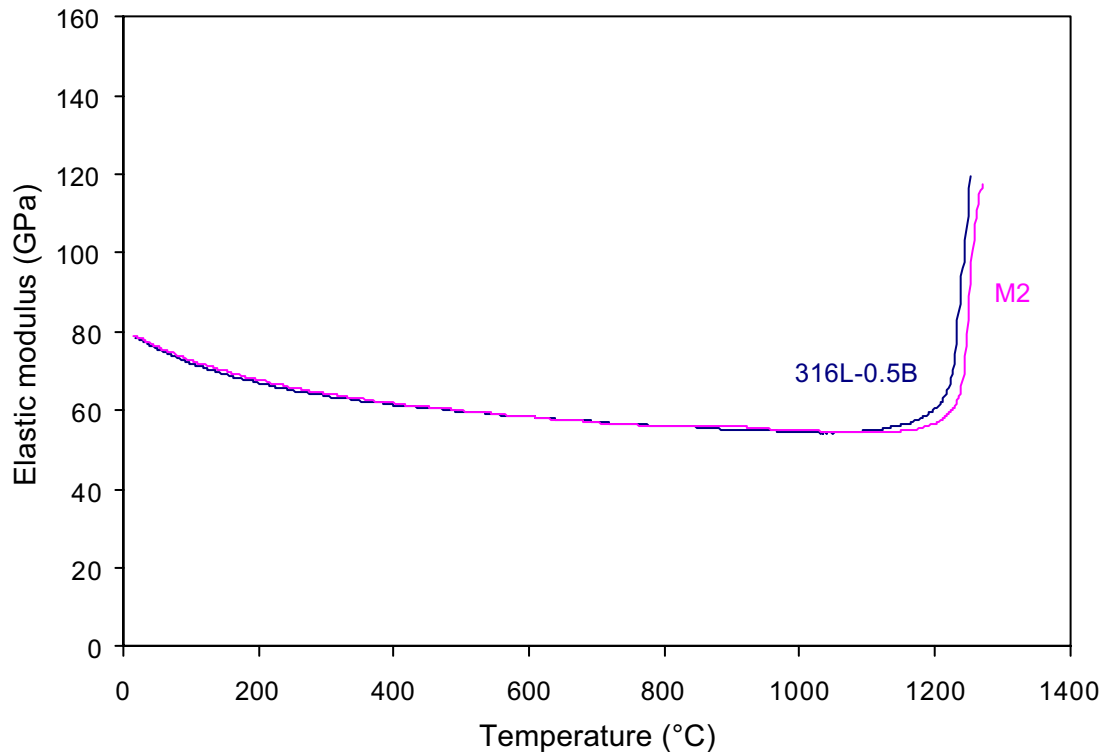

Figure 8. Temperature dependence of the elastic moduli of M2 and 316L-0.5B.

The maximum hoop stress is plotted in Figure 9 as a function of temperature using the elastic moduli data along with the shrinkage data for M2 and 316L-0.5B from Figure 1. Since the 316L-0.5B densifies more rapidly than the M2, it is used for the outer ring, which helps to ensure constant contact and good bonding. Also, this places the maximum tensile hoop stress at the interface where it is lower in magnitude than if it were at the inner diameter. A comparison of Figure 9 and Figure 7 shows that the hoop stress stays below the *in situ* strength at all temperatures, suggesting that Bi-MIM components can be processed from these two materials.
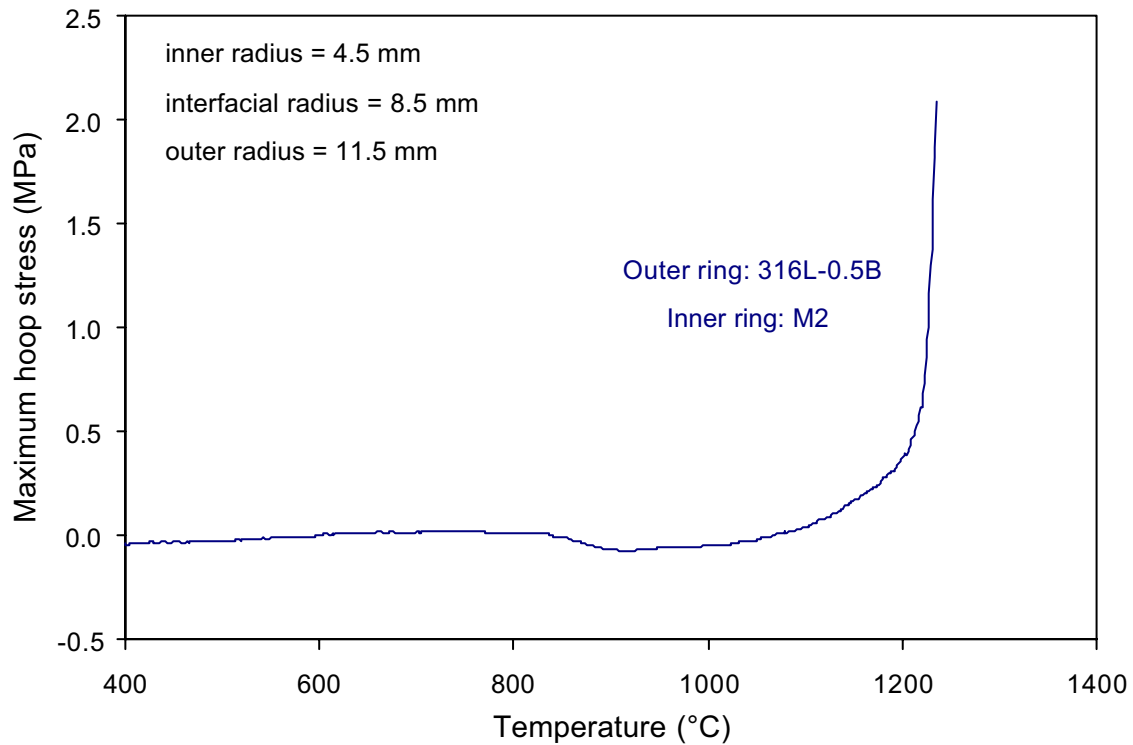
Figure 9. Maximum hoop stresses induced during co-sintering of concentric rings of M2 (inner ring) and 316L-0.5B (outer ring).

DEMONSTRATION COMPONENT

An example bimaterial component consisting of an inner ring of M2 tool steel and an outer ring of 316L-0.5B austenitic stainless steel is shown in Figure 10. This component was two-color injection molded, thermally debound, and sintered at 1235°C. Sintering at 1245°C resulted in distortion of the 316L-0.5B outer ring due to the high amount of liquid that formed at this temperature. A slight reduction in boron content of the 316L is needed to obtain optimal properties and shape retention at 1245°C rather than 1235°C. As predicted by the co-sintering model, no radial cracks were formed in either case. Because of the similarities in the chemistries of the two steels, a good metallurgical bond results as shown in Figure 11. However, the M2 grain size is much larger than shown in Figure 5 and liquid films are present at the grain boundaries. This enhanced grain growth is likely due to diffusion of the boron across the interface.

Figure 10. A demonstration bi-material component consisting of a wear resistant M2 tool steel inner ring surrounded by a ductile 316L-0.B outer ring.
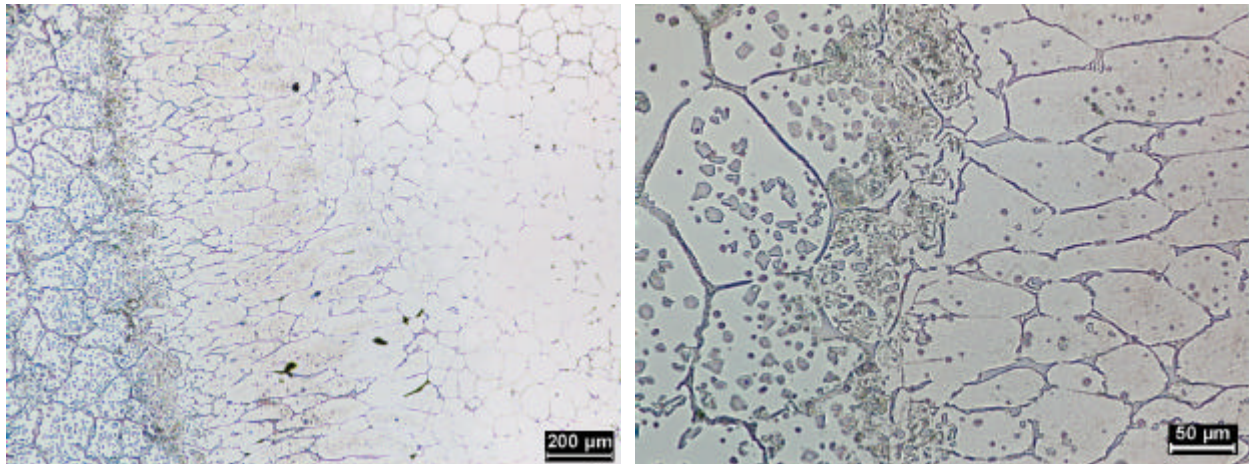

Figure 11. Optical micrographs at 50X (left) and 200X (right) of the interface of M2 and 316L-0.5B co-sintered at 1245°C.

CONCLUSIONS

Boron additions of 0.5 wt.% enhance the sintering of 316L stainless steel such that it has similar densification behavior to M2 tool steel. Strength, density, and hardness after sintering 316L-0.5B at 1245°C are all improved in comparison to 316L sintered at 1330°C. Ductility is reduced to 15%, but this is still acceptable for many applications. M2 sintered at 1245°C shows high strength and can achieve a hardness of 59 HRC after heat treating. The hoop stresses generated during co-sintering of M2 and 316L-0.5B concentric rings do not exceed the *in situ* strengths of the materials, allowing for the fabrication of demonstration Bi-MIM components with a unique combination of wear resistance and toughness.

REFERENCES

[1] Tan, L.K., Baumgartner, R., and German, R.M., "Powder Injection Molding of Bi-Metal Components," *Advances in Powder Metallurgy and Particulate Materials*, vol. 4, compiled by W.B. Eisen and S. Kassam, Metal Powder Industries Federation, Princeton, NJ, 2001, pp. 191-198.
[2] Lim, K.L., Tan, L.K., Tan, E.S., and Baumgartner, R., "Method to Form Multi-Material Components," U.S. Patent No. 6,461,563.
[3] Heaney, D.F., Suri, P., and German, R.M., "Two-Color Injection Molding of Hard and Soft Metal Alloys," *Proceedings of the 2002 International Conference on Functionally Graded Materials: Technology Leveraged Applications*, compiled by R.G. Ford and R.H. Hershberger, Metal Powder Industries Federation, Princeton, NJ, 2002, pp. 105-115.
[4] "Sintering Mechanisms in Vacuum Sintered M2 and T15 High Speed Steel Powders," *Metal Powder Report*, 1988, vol. 43, no. 3, pp. 177-184.
[5] Myers, N.S., and German, R.M., "Supersolidus Liquid Phase Sintering of Injection Molded M2 Tool Steel," *International Journal of Powder Metallurgy*, vol. 35, no. 6, 1999, pp. 45-51.
[6] Tandon, R. and German, R.M., "Sintering and Mechanical Properties of a Boron-Doped Austenitic Stainless Steel," *International Journal of Powder Metallurgy*, vol. 34, no. 1, 1998, pp. 40-49.
[7] Xu, X., Lu, P., and German, R.M., "Densification and Strength Evolution in Solid-State Sintering Part II," *J. of Mater. Sci.*, vol. 37, 2002, pp. 117-26.
[8] Bickford, W.B., *Advanced Mechanics of Materials*, Addison-Wesley, Menlo Park, CA, 1998.